

Generating Realtime Motion Plans from Complex Natural Language Commands Using Dynamic Grounding Graphs

Jae Sung Park and Biao Jia and Mohit Bansal and Dinesh Manocha

Abstract We present an algorithm for combining natural language processing (NLP) and realtime robot motion planning to automatically generate safe robot movements. We present a novel method to map the complex natural language commands into appropriate cost function and constraint parameters for optimization-based motion planning. Given NLP commands, we generate a factor graph named Dynamic Grounding Graph (DGG). The coefficients of this factor graph are learned based on conditional random fields and used to dynamically generate the constraints for motion planning. We directly map the cost function to the parameters of the motion planner to generate collision-free and smooth paths in complex scenes with moving obstacles. We highlight the performance of our approach in a simulated environment as well as a human interacting with a 7-DOF Fetch robot with complex NLP commands.

1 Introduction

In human-robot interaction (HRI), natural language processing (NLP) has been used as one of the interfaces to communicate human’s intent to a robot [1, 2, 3, 4]. There is substantial work in this area that has focused on simple commands or tasks for robot manipulation, such as pick and place objects. As robots are increasingly used in complex scenarios and applications, it is important to develop a new generation of motion planning and robot movement techniques that can respond appropriately to diverse and free-form NLP commands for HRI. This includes automatic parsing of rich and complex natural language commands and generate appropriate robot actions. For example, humans frequently issue commands that include sentences with orientation-based constraints such as “put a bottle on the table and keep it

Jae Sung Park, Biao Jia, Mohit Bansal and Dinesh Manocha
University of North Carolina at Chapel Hill, USA, e-mail: {jaesungp, biao, mbansal,dm}@cs.unc.edu

upright”, or “move the knife but don’t point it towards people”, or sentences with velocity-based constraints such as “move slowly when you are human gets close”. In order to generate robot actions and movements in response to such complex natural language commands, we need to deal with two kinds of challenges:

- Correct interpretation of motion-based natural language commands and their semantics, especially taking into account the environment and the context. For example, a human may say “move a little to the left”, or “do not move like this”, then the planner needs to learn the correct interpretation of these commands with novel adjectives, adverbs, and negation.
- The real-time motion planner needs to generate appropriate trajectories based on these complex natural language commands. This includes appropriately setting up the motion planning problem based on advanced constraints (e.g., orientation, velocity, smoothness, and avoidance) and computing smooth and collision-free paths.

Motion planning has been extensively studied in robotics and related areas for more than four decades. There is a large body of work to compute collision free paths between two configurations or perform clearly specified tasks, that take into account various constraints corresponding to robot kinematics and dynamics, uncertainty or the environment. However, current motion planning algorithms used with NLP need to deal with additional constraints that arise due to the use of complex commands corresponding to negation, orientation, velocity, etc.

Main Results: We present a novel approach, called Dynamic Grounding Graphs (DGG), to map natural language commands to appropriate optimization-based motion planning formulation in a dynamic environment. Our planner uses constrained optimization to compute a high-DOF collision-free trajectory for the robot and we construct parametric constraints based on interpretation of natural language semantics. The novel contributions of our work include:

- The input natural language commands for a robot are processed by rule-based parser to generate a parse tree. We present a mapping scheme between the parse tree and parametric constraints in optimization-based planner.
- A learning algorithm to compute the mapping efficiently. In order to deal with complex natural language commands, we use DGG, an extended Generalized Grounding Graphs (G^3) [1], based on Conditional Random Field (CRF).
- Real-time trajectory optimization using the mapped cost functions. The real-time motion planner computes the best robot trajectory in terms of a taking into account different constraints including smoothness, collision avoidance, safety, etc. The cost function parameters are adjusted at every timestep, depending on natural language commands and the position of the obstacles in the environment, so that the motion planner can compute a locally optimal trajectory.

We highlight the performance of our algorithms in a simulated environment as well as on a 7-DOF Fetch robot operating next to a human in a safe manner. Our approach can handle a rich set of natural language commands and generate appropriate paths in realtime. These include complex commands such as picking (e.g.,

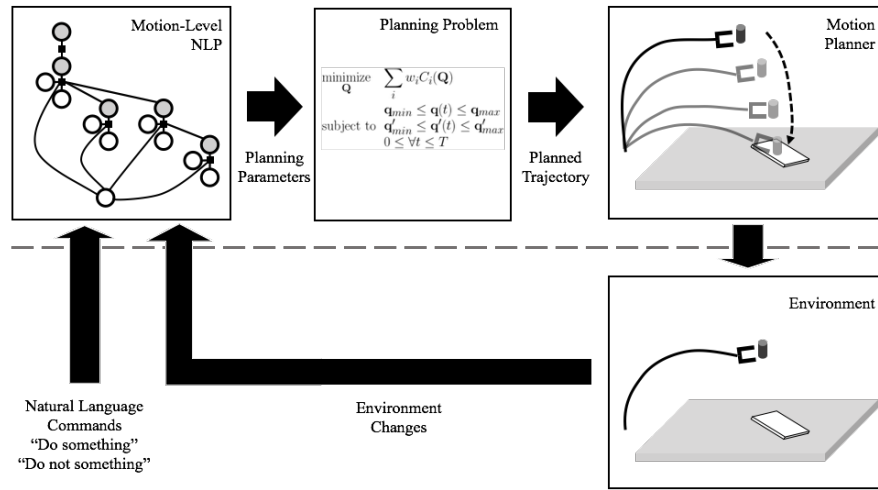


Fig. 1 Overall pipeline of our approach that highlights the NLP parsing module and the realtime motion planner. Above the dashed line, the following components are highlighted from left to right: Dynamic Grounding Graphs (DGG) that are used to parse and interpret the natural language commands, generation of optimization-based planning formulation with appropriate constraints and parameters using our mapping algorithm, and uses a realtime optimization-based motion planner for dynamic environments. We highlight the high-level interface below the dashed line. As the environment changes or new natural language commands are given, our approach changes the specification of the constraints for the optimization-based motion planner and generates the new motion plans in realtime.

“pick up a red object near you”), correcting the motion (e.g., “don’t pick up that one” or negation “don’t put it on the book”).

2 Related Work

Most algorithm used to map the natural language instruction to robot actions tends to separate the problem into two parts, the parsing part and motion planning computation. In this section, we give a brief overview of prior work in these areas.

2.1 Natural Language Processing

Kollar et al. [1] present a probabilistic graphical learning model called Generalized Grounding Graphs or G^3 , by which the robot interprets and grounds natural language commands to the physical world. The graph is defined based in a syntactic parse structure of the command, enabling the system to associate parts of the command with objects, events, and locations in the external world to which they refer.

Howard et al. [2] reduced the search space by modifying the G^3 graph structure by adding all possible grounding nodes (meanings of word phrases) and optimizing the correspondence variables (indicating the word phrase and the grounding matches correctly).

Other related work in language grounding of task instructions includes Branavan et al. [3, 5], who applied reinforcement learning to learn the mapping from natural language instructions to sequences of executable actions. Reinforcement learning based method requires little annotated data, but the search space can be very large when applied to motion planning for the robot arm. Matuszek et al. [4] use a statistical machine translation model to map the natural language instructions to a path description language to follow directions in a robot navigation problem. Duvallet et al. [6] exploit imitation learning to train the model via demonstrations of humans following directions.

Our approach is inspired by [1] and [2] with respect to the linguistic parse structure and the probabilistic graphical model. However, we extend these methods so that they can be directly integrated with optimization-based planners in terms of using appropriate constraints.

2.2 Robot Motion Planning in Dynamic Environments

In order to generate collision-free motion plans in dynamic environments, many re-planning algorithms have been suggested. Fox et al. [7] proposed the dynamic window approach that searches for optimal velocity in a short period of time window to avoid dynamic obstacles. Optimization-based motion planners [8, 9, 10, 11] solve a constrained optimization problem to generate smooth and collision-free robot paths. These optimization-based planners can be adapted to other planning tasks by adding cost functions and constraints in the optimization formulation. However, it is hard and tedious to manually tune many parameters and the goal is to generate such constraints and parameters automatically.

There is some work on integrating optimization-based motion planning with NLP in 2D workspaces. Silver et al. [12]. developed an algorithm of learning navigation cost functions from demonstration. Howard et al. [2] used probabilistic graphical model to generated motion planning constraints in 2D navigation problem. As compared to these methods, our approach can handle 3D workspaces and high-dimensional configuration spaces to generate robot motions based on complex NLP commands.

2.3 Robot Motion Planning for Human-Robot Interaction

There is considerable work on generating safe motion plans for robots operating next to humans. Some methods use the notion of social acceptability [13] or legi-

bility [14]. Mainprice and Berenson [15] constructed occupancy map for each voxels in the workspace to explicitly represent whether a voxel is likely to be occupied by humans, so that motion planners can generate collision-free robot paths. Other techniques focus on efficiency in human-robot collaborative tasks. Markov Decision Processes (MDP) are widely used to compute the best robot action policies [16, 17, 18]. Optimization-based online replanning [11, 19] has been successfully used for high-DOF robots in dynamically changing environments. These algorithms interleave planning and trajectory execution timesteps and incrementally compute the solution to perform robot tasks and we use a similar framework.

3 Overview

We first introduce the notation and terminology used in the paper and give an overview of our natural language processing and motion planning algorithms.

3.1 Natural Language Processing

From an input natural language command, we construct a factor graph, as shown in the left column of Fig. 2, based on parsing of the command. For each node of the parse tree, we generate three types of node: word phrase node λ , grounding node γ , and correspondence node ϕ .

The input sentence Λ is parsed by NLTK library [20]. Word phrase of each node in the parse tree is denoted as λ_i for $i = 1, 2, \dots$. Children of λ_i are $\lambda_{i1}, \dots, \lambda_{im}$. The root node of parse tree is λ_1 . For example, in Fig. 2(a), the input sentence is “Put the cup on the table”. The parse tree has the root word phrase $\lambda_1 = \text{“Put”}$, and its noun $\lambda_2 = \text{“the cup”}$ and the preposition $\lambda_3 = \text{“on”}$ are the children nodes of the root node. The noun phrase $\lambda_4 = \text{“the table”}$ is the child node of λ_3 . Similarly, in Fig. 2(b), the command “Don’t put it there” is decomposed into 4 noun phrase nodes. The word phrase $\lambda_1 = \text{“Don’t”}$ is a negation of the verb, its child node $\lambda_2 = \text{“put”}$. $\lambda_3 = \text{“it”}$ and $\lambda_4 = \text{“there”}$ are the children nodes of λ_2 . Note that the parse tree is different from the parse tree in Fig. 2(a).

We first compute the groundings γ_i of each word phrase λ_i . Grounding of each word phrase is the mapping from the word phrase to the meaning of it in the real world. Groundings can be objects, locations, motions, tasks or constraints. In our model, the grounding γ_i depends on its work phrase λ_i and children grounding nodes $\gamma_{i1}, \dots, \gamma_{im}$, where the tree structure of grounding nodes follow the parse tree. For example, in Fig. 2(a), the groundings of $\lambda_2 = \text{“the cup”}$ and $\lambda_4 = \text{“the table”}$ indicate the objects (the cup and the table) in the environment. The grounding of $\lambda_3 = \text{“on”}$, with consideration of $\gamma_4 = \text{the table}$, indicates the region *the surface of the table*. The grounding of $\lambda_1 = \text{“Put”}$ is the task of moving *the cup on the surface of the*

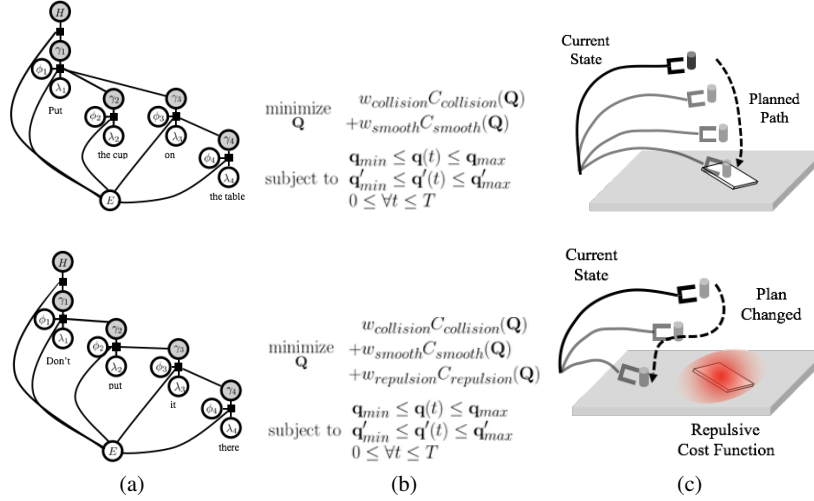


Fig. 2 Factor graphs for different commands: In the environment in the right column, there is a table and a thin rectangular object on it. A robot arm is moving a cup on the table but we want it to avoid moving over the book based on NLP commands. (a) The command “Put the cup on the table.” is given, and the factor graph is constructed (left). Appropriate cost functions for the task are assigned to the motion planning algorithm (middle) and used to compute the robot motion (right). (b) As the robot gets close to the nook, another command “Don’t put it there.” is given; A different factor graph is constructed (left) with different cost functions (middle) and computed path (right).

table, and it is the task the robot should accomplish. In Fig. 2(b), the negation part $\lambda_1 = \text{“Don’t”}$ is interpreted as a constraint that the robot should not do something.

Correspondence node ϕ_i indicates the correct matching between the word phrase λ_i and the grounding γ_i . It is a binary variable; ϕ_i is *true* if the word phrase and the grounding correctly matches and *false* if not. For example, in Fig. 2(a), if the grounding for $\lambda_2 = \text{“the cup”}$ is $\gamma_2 = \text{the cup in the environment}$, they match correctly and so $\phi_2 = \text{true}$. However, if the grounding node is predicted incorrectly like $\gamma_2 = \text{the table}$ or $\gamma_2 = \text{(putting task)}$, then it does not correspond to “the cup” so $\phi_2 = \text{false}$. The correspondence nodes are useful in the machine learning framework. In training step, a ground-truth data sample contains the correct groundings γ_i , thus all correspondence nodes are $\phi_i = \text{true}$. We can synthesize more data samples by assigning wrong groundings to some γ_i and set $\phi_i = \text{false}$.

Our primary novel goal is to compute the best cost function parameters that we directly use in the optimization-based motion planning, corresponding to a mapping from the input natural language commands. We denote $H \in \mathbb{R}^h$, a real vector of size h , as a collection of cost function parameters, where the size h , the number of cost function parameters, depends on what types of cost functions are used.¹ We define

¹ In this paper, we set $h = 22$ to fully specify the smoothness, end-effector position, end-effector orientation, end-effector speed and repulsion cost functions. It is a sum of 5 for weights, 16 for positions and orientations, and 1 for an exponential constant.

many types of cost functions, such as the collision avoidance, robot smoothness, robot end-effector speed, target positions and target orientations. Each cost function has its weight and other cost function parameters if necessary. For example, the robot end-effector speed cost function has parameters corresponding to the direction and the magnitude of the speed which impose a constraint on the final computed trajectory. If the weight of end-effector speed cost function is higher than others, then it takes a large portion of the overall object function in the optimization formulation and thus the cost function affects more to the planned path. If the weight is low, then the end-effector speed cost will be compromised and affect less to the planned path. We want the robot to avoid collisions in any case, so we set the weight of collision avoidance cost to 1, and other cost function weights are normalized by this weight. The details of cost function parameters are explained in Section 5. In Fig. 2, the resulting constraint based motion planning problems are shown in the middle column. In (a), we use collision avoidance cost function as default, smoothness cost function and the target location cost function. The target location, whose 3D coordinates are the cost function parameters, is set on the surface of the table. The cost function parameter node H contains the weights of them and the 3D coordinate of target location. In (b), where a new “Don’t” command is given, a repulsion cost function is added. Thus, the cost function weight and the location of repulsion source (below the robots end-effector position) are added to H .

3.2 Robot Configurations and Motion Planning

We denote a single configuration of the robot as a vector \mathbf{q} that consists of joint-angles. A configuration at time t , where $t \in \mathbb{R}$, is denoted as $\mathbf{q}(t)$. We assume $\mathbf{q}(t)$ is twice differentiable, and its derivatives are denoted as $\mathbf{q}'(t)$ and $\mathbf{q}''(t)$. The n -dimensional space of configuration \mathbf{q} is the configuration space \mathcal{C} . We represent each link of the robot as R_i . The finite set of bounding box for link R_i is B_i . The links and bounding boxes at a configuration \mathbf{q} are denoted as $R_i(\mathbf{q})$ and $B_i(\mathbf{q})$, resp.

For a planning task with a given start configuration \mathbf{q}_0 and derivative \mathbf{q}'_0 , the robot’s trajectory is represented by a matrix \mathbf{Q} ,

$$\mathbf{Q} = \begin{bmatrix} \mathbf{q}_0 & \mathbf{q}_1 & \mathbf{q}_{n-1} & \mathbf{q}_n \\ \mathbf{q}'_0 & \mathbf{q}'_1 & \cdots & \mathbf{q}'_{n-1} & \mathbf{q}'_n \\ t_0 = 0 & t_1 & t_{n-1} & t_n = T \end{bmatrix}.$$

The robot trajectory passes through the $n + 1$ waypoints q_0, \dots, q_n , which will be optimized by an objective function under constraints in the motion planning formulation. Robot configuration at time t is interpolated from two waypoints. Formally, for j such that $t_j \leq t \leq t_{j+1}$, the configuration $\mathbf{q}(t)$ and derivative $\mathbf{q}'(t)$ are cubically interpolated using $\mathbf{q}_j, \mathbf{q}'_j, \mathbf{q}_{j+1}$ and \mathbf{q}'_{j+1} .

The i -th cost functions of the motion planner are $C_i(\mathbf{Q})$. 6 different cost functions we used in this paper are listed in Section 5. Our motion planner solves an opti-

mization problem with a non-linear cost functions and linear joint limit constraints to generate robot trajectories for time interval $[0, T]$,

$$\begin{aligned} & \underset{\mathbf{Q}}{\text{minimize}} && \sum_i w_i C_i(\mathbf{Q}) \\ & \text{subject to} && \mathbf{q}_{min} \leq \mathbf{q}(t) \leq \mathbf{q}_{max}, 0 \leq \forall t \leq T. \\ & && \mathbf{q}'_{min} \leq \mathbf{q}'(t) \leq \mathbf{q}'_{max} \end{aligned} \quad (1)$$

In the optimization formulation, C_i is the i -th cost function and w_i is the weight of the cost function. The collection of cost function parameters include the cost function weights w_i , and other required information specified in some cost functions. For example, x , y and z coordinates target position are the parameters we want to find, for the end-effector position cost function $C_{position}$ (explained in Section 5).

4 Dynamic Grounding Graphs

Our work builds on the idea of Generalized Grounding Graphs (G^3) model and Distributed Correspondence Graph (DCG) model [2], and extend it to generate the appropriate learning model. Our goal of learning natural language commands is to find a mapping from a natural language sentence Λ to the cost function parameters H , given the robotic environment E , where the robot is working. E is a representation for the environment composed of obstacle positions, orientations, and robot's configuration. From the environment description, feature vectors are constructed in the factor graph. H is a real-valued vector that contains all cost function parameters used in the optimization-based motion planner. It also includes the weights of different types of cost functions used in the optimization formulation. For example, the end-effector position cost function (Equation (2)) requires 3D coordinates of target position as parameters. The repulsion cost function (Equation (3)) requires the repulsion source position and the constant in the exponential function.

We use a probabilistic model for H , Λ and E . Finding the best cost parameters is posed as an optimization problem:

$$\underset{\mathbf{H}}{\text{maximize}} \quad p(H|\Lambda, E).$$

However, modeling the probability function without decomposing the variables and some independence assumptions is hard due to the high-dimensionality of H , Λ and E and the dependencies between them. To simplify the problem, the natural language sentence is decomposed into n word phrases based on a parse tree, i.e.

$$p(H|\Lambda, E) = p(H|\lambda_1, \dots, \lambda_n, E).$$

Like G^3 , we introduce the intermediate groundings γ_i of word phrases λ_i , and correspondence variable ϕ_i . The correspondence variables ϕ_i is a binary random variable.

The value 1 indicates that the word phrase λ_i correctly corresponds to the grounding γ_i . 0 means an incorrect correspondence.

We assume conditional independence of the probabilities to construct a factor graph (see left column of Fig. 2). With the independence assumptions, a single factor is connected to a word phrase node and its children grounding nodes containing information about the sub-components. These independence assumptions simplify the problem and make it solvable by efficiently taking advantage of the tree structure of the probabilistic graphical learning model. Formally, the root grounding node γ_1 contains all the information about robot’s motion. The factor connecting γ_1 and H means that from the root grounding node, the cost function parameters H are optimized without any consideration of other nodes. Other factors connect γ_i , ϕ_i , λ_i , children grounding nodes γ_j , and the environment E , where parent-child relationship is based on parse tree constructed from the natural language sentence. This graph representation corresponds to the following equation:

$$p(H|\lambda_1, \dots, \lambda_n, E) = p(H|\gamma_1, E) \prod_i p(\gamma_i|\lambda_i, \phi_i, \gamma_{i1}, \dots, \gamma_{im}, E).$$

For the root factor connecting H , γ_1 and E , we formulate the continuous domain of H . We compute the Gaussian Mixture Model (GMM) on the probability distribution $p(H|\gamma_1, E)$ and model our probability with non-root factors as following:

$$p(\gamma_i|\lambda_i, \phi_i, \gamma_{i1}, \dots, \gamma_{im}, E) = \frac{1}{Z} \psi_i(\gamma_i, \lambda_i, \phi_i, \gamma_{i1}, \dots, \gamma_{im}, E) = \frac{1}{Z} \exp(-\theta_i^T f(\gamma_i, \lambda_i, \phi_i, \gamma_{i1}, \dots, \gamma_{im}, E)),$$

where Z is the normalization factor, ψ_i is the feature function, and θ_i and f is the log-linearization of the feature function. The function f generates a feature vector, given a grounding γ_i , a word phrase λ_i , a correspondence ϕ_i , children groundings γ_j and the environment E .

- *Word phrases.* The feature vector includes binary-valued vectors for the word and phrases occurrences, and Part of Speech (PoS) tags. In particular, there is a list of words that could be encountered in the training dataset, like $\{put, pick, cup, up, there, \dots\}$. If the word phrase contains the word *put*, then the occurrence vector at the first index is set to 1 and others are set to 0. If the word phrase is *pick up*, then the occurrence vector values at the second and the fourth is set to 1 and others to 0. It also includes real-valued word similarities between the word and the pre-defined seed words. The seed words are the pre-defined words that the users expect to encounter in the natural language commands. We used Glove word2vec [21] to measure cosine-similarity (i.e. the inner product of two vectors divided by lengths of the vectors) between the words. The measurement indicates the words are similar if the similarity metric value is near 1, have opposite meaning if similarity metric is near -1 and weak relationship if it is near 0. This provides more flexibility to our model, especially when it encounters new words that are not trained during the training phase.
- *Robot states:* From the robot state, we collect the robot joint angles, velocities, the end-effector position, the end-effector velocity, etc. This information can affect the cost function parameters even while processing the same natural

language commands. For example, if the robot is too close to a human under the current configuration, then the cost function for end-effector speed C_{speed} or smoothness $C_{smoothness}$ will be adjusted so that the robot does not collide with the human. We also store information about the objects that are close to the robot. They include object type, position, orientation, shape, dimension, etc.

As we construct the factor graph, we build a learning model on it and use that for training and inferring the meaning of given commands. In particular, we use Conditional Random Fields (CRF), a learning model for factor graphs. During the training step of CRF, we solve the optimization problem of maximizing the probability of the samples in the training dataset over the feature coefficients θ_i for every parse tree structure. Multiplying Eq. (4) for all training samples, the optimization problem becomes

$$\text{maximize}_{\theta_1, \dots, \theta_n} \prod_k p(H^{(k)} | \gamma_1^{(k)}, E^{(k)}) \prod_i \frac{1}{Z^{(k)}} \exp(\theta_i^T f(\gamma_i^{(k)}, \lambda_i^{(k)}, \phi_i^{(k)}, \gamma_{i1}^{(k)}, \dots, \gamma_{im}^{(k)}, E^{(k)})),$$

where superscripts $(k) = 1 \dots D$ mean the indices of the training samples. This is a tree-structured CRF problem.

At the inference step, we used the trained CRF factor graph models to find the best groundings Γ and the cost function parameters H by solving the CRF maximization problem

$$\text{maximize}_{H, \gamma_1, \dots, \gamma_n} \prod_k p(H | \gamma_1, E) \prod_i \frac{1}{Z} \exp(\theta_i^T f(\gamma_i, \lambda_i, \phi_i, \gamma_{i1}, \dots, \gamma_{im}, E)).$$

Because the nodes $H, \gamma_1, \dots, \gamma_n$ being optimized has a tree structure in the factor graph, we can solve the optimization problem efficiently using dynamic programming. Each factor depends on its parent and children varying variables and other fixed variables connected to it. This implies that we can solve the sub-problems in a bottom-up manner and combine the results to solve the bigger problem corresponding to the root node.

5 Real-time Trajectory Planning With NLP Input

We present our realtime optimization-based planning algorithm that handle complex NLP commands. The overall optimization formulation is given in Eqn. 1 in Sec. 3.2. In order to formulate the constraints, we use the following cost functions:

Collision avoidance: By default, the robot should always avoid obstacles.

$$C_{collision}(\mathbf{Q}) = \int_0^T \sum_i \sum_j \text{dist}(B_i(t), O_j)^2 dt,$$

where $dist(B_i(t), O_j)$ is the penetration depth between a robot bounding box $B_i(t)$ and an obstacle O_j . As it is a default cost function, we set the weight of this cost function 1, and changes the weights of other types of cost functions accordingly.

Smoothness: We penalize the magnitude of robot’s joint angle speeds to make the trajectory smooth. This correspond to the integral of first derivative of joint angles over the trajectory duration. This function is useful when we need to control the speed of the robot. When the robot should operate at a low speed (e.g. when a human is too close), or we don’t want abrupt moves (e.g. for human safety), the smoothness cost can have high weights so that the robot moves slowly without jerky motions.

End-effector position: Usually, a user specifies the robot’s target position so that the robot reaches a goal position. This cost function penalizes the squared distance between robot’s end-effector and the target position over the trajectory duration.

$$C_{position}(\mathbf{Q}) = \int_0^T \|\mathbf{p}_{ee}(t) - \mathbf{p}_{target}\|^2 dt, \quad (2)$$

where $\mathbf{p}_{ee}(t)$ is the robot end-effector position at time t , and \mathbf{p}_{target} is the target position. The target position \mathbf{p}_{target} is considered as a cost function parameter. In the NLP algorithm, a position grounding node encodes the target position parameter. It can be a 3D position or the current object position in the environment. Typically, the target position is specified by object names in the sentence, such as “*pick up the cup*” or “*move to the box*”. In these cases, the grounding nodes for “*the cup*” and “*the box*” are interpreted as the current 3D coordinates of target positions, which are the parameters of this cost function.

End-effector orientation: Robotic manipulation tasks are sometimes constrained by the end-effector orientation. This cost function penalizes the squared angular differences between end-effector orientation and the target orientation over the trajectory duration.

$$C_{orientation}(\mathbf{Q}) = \int_0^T \text{angledist}(\mathbf{q}_{ee}(t), \mathbf{q}_{target})^2 dt \quad C_{upvector}(\mathbf{Q}) = \int_0^T \text{angledist}(\mathbf{n}_{up}(t), \mathbf{n}_{target})^2 dt,$$

where $\mathbf{q}_{ee}(t)$ is the quaternion representation of the robot end-effector’s orientation at time t , \mathbf{q}_{target} is the orientation that we want the robot to maintain its end-effector orientation to be, \mathbf{n}_{up} is the normal up-vector of robot’s endeffector, and \mathbf{n}_{target} is the target up-vector. Similar to *End-effector position* cost, the target orientation \mathbf{q}_{target} is the cost function parameters. The target orientation usually depends on the object the robot picked up. E.g., when the robot is doing a peg-hole insertion task under a given command “*insert that into the hole*”, the orientation of robot’s end-effector \mathbf{q}_{ee} should be constrained near the hole. If the robot arm is holding a cup of water, it should be upright so as to not spill the water. In this case, \mathbf{n}_{target} is set to $(0, 0, 1)$.

End-effector speed: It penalizes the robot’s endeffector speed and direction:

$$C_{speed}(\mathbf{Q}) = \int_0^T \|\mathbf{v}_{ee}(t) - \mathbf{v}_{target}\|^2 dt,$$

where $\mathbf{v}_{ee}(t)$ is the robot end-effector speed at time t , and \mathbf{v}_{target} is the target speed. The parameters of this cost function is \mathbf{v}_{target} . In some cases, it is required to restrict

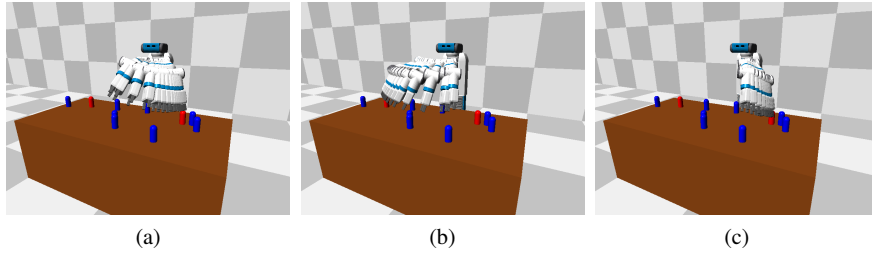


Fig. 3 The simulated Fetch robot arm is reaching to one of the two red objects and we highlight the positions along the computed trajectory. (a) When a command “*pick up one of the red object*” the robot moves to the right red object. Because the user doesn’t specify which object to pick among the two, the robot chooses the one based on the DGG algorithm. (b) If the user doesn’t want the robot to pick up the right object, it uses a command “*don’t pick up that one*”. Our DGG algorithm dynamically changes the cost function parameters so that the robot picks the other object. (c) The robot approaches the right object and stops as there are no more commands.

the robot’s end-effector velocity. For example, a user wants to pick up a cup filled with water and doesn’t want to spill it. Spilling can be prevented by limiting the end-effector speed to be slow. Or the user can guide the motion by using natural language commands like “*Move left, then move around the obstacle*” to compute a better trajectory.

Repulsion: The repulsion functions are commonly used as potential fields

$$C_{repulsion}(\mathbf{Q}) = \int_0^T \exp(-c \|\mathbf{p}_{ee}(t) - \mathbf{p}_r\|) dt, \quad (3)$$

where \mathbf{p}_r is the position where we don’t want the robot to move to. The coefficient $c > 0$ plays the role of how much is the cost affected by $\|\mathbf{p}_{ee}(t) - \mathbf{p}_{repulsive}\|$, the distance between the end-effector position and the repulsion source. The cost function is maximized at which the end-effector position is exactly at the repulsion source, and decreases as the distance between the end-effector and the repulsion position increases. For example, if the command is “*Don’t put the cup on the laptop*”, we can define a repulsion cost with the laptop position as the repulsion source. The cost function is inversely proportional to the distance between the end-effector and the laptop.

6 Implementation and Results

We have implemented our algorithm and evaluated its performance in a simulated environment and a 7-DOF Fetch robot. All the timings are generated on a multi-core PC.

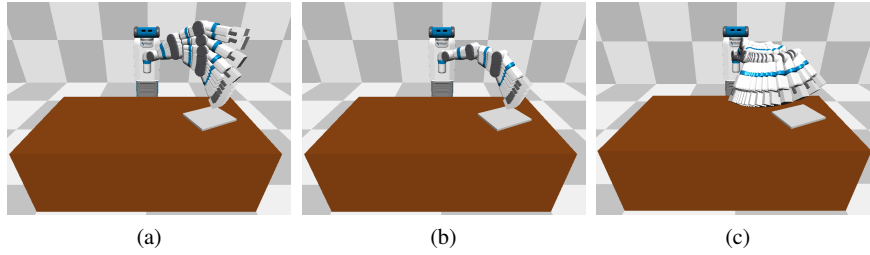


Fig. 4 In this simulated environment, the human asks the robot to “put the cube on table” (a); As it approaches the laptop (b), the human uses a negation NLP command “don’t put it there”, so the robot places at a different location (c).

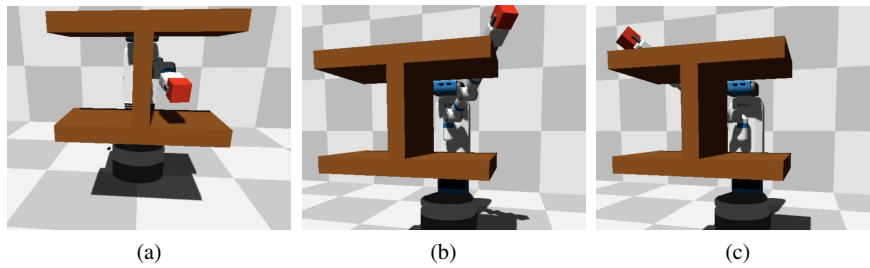


Fig. 5 A 7-DOF Fetch robot is operating in a simulated environment avoiding an obstacle. (a) In traditional optimization-based motion planner, the planner gets stuck at a local minimum. (b),(c) Using natural language commands as guidance, the user guides the robot out of the minimal and towards the goal position.

We have evaluated the performance in complex environments composed of multiple objects and local minima. Based on the NLP commands, the robot decides to pick an appropriate object or is steered towards the goal position in a complex scene (see Fig. 5. In particular, the NLP commands are used to guide the robot by the user by using commands such as “*move right*”, “*move up*”, “*move left*” or “*move down*”. For each such commands, we compute the appropriate cost functions.

We also integrated our NLP-based planner with ROS and evaluated its performance on the 7-DOF Fetch robot. In a real-world setting, we test its performance on different tasks corresponding to: (1) move a soda can on the table from one position to the other; (2) not move it over the book. With a noisy point cloud sensor on the robot, the thin book is not recognized as a separate obstacle by the robot, though the human user wants the robot to avoid it. Our NLP algorithm evaluates the meaning of the commands and generates appropriate cost function and constraint parameters for the real-time motion planner. In Fig. 6, the two sub-tasks are specified in one sentence at the beginning, as “*move the can on the table, but don’t put it on the book*”. The cost function is used to move the robot’s end-effector to the surface of the table. Another cost function penalizes the distance between the book and the

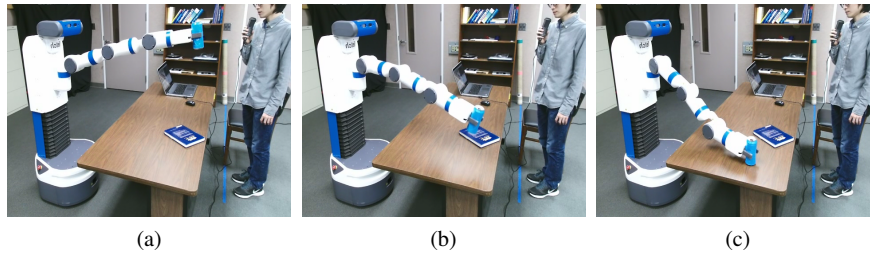


Fig. 6 The Fetch robot is taking realtime commands from the human and moves the soda can on the table.

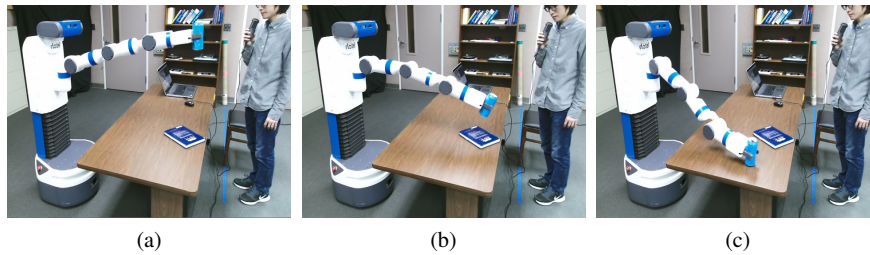


Fig. 7 The Fetch robot is moving a soda can on a table. Initially the user gives the “pick and place” command. However, when the robot gets closer to the book, the person says “*don’t put it there*” and the robot avoids the book using appropriate cost functions and optimization.

end-effector. In Fig. 7, only the first sub-task is given at the beginning. This results in the robot moving the can on the book. As the robot gets too close to the book, the person says “*stop*”, then says “*don’t put it there.*” The robot recomputes the cost functions and avoids the region around the book.

7 Analysis and Benefits

In this section, we analyze the performance of our approach and highlight its benefits over prior methods. We evaluated the end-to-end performance of our approach including the NLP, mapping and the motion planning modules on different benchmarks. We evaluated the performance based on the following metrics:

- *Success Rate*: is the ratio of successful task completion among all trials. Failure includes colliding with the obstacles due to incorrect mapping of cost function parameters, violating constraints specified by natural language commands, or not completing the task due to other reason.

# Training Data	Success Rate	Trajectory Duration	Trajectory Smoothness Cost
1,000	5/10	23.46s (5.86s)	8.72 (5.56)
3,000	9/10	16.02s (3.28s)	2.56 (0.64)
10,000	10/10	13.16s (1.24s)	1.21 (0.32)
30,000	10/10	12.81s (0.99s)	0.78 (0.12)
100,000	10/10	12.57s (0.97s)	0.72 (0.10)

Table 1 Planning performances with varying number of training data for the scenario in Fig. 3. We report the success rate over the number of trials, and the average and standard deviations (in the last two columns) of trajectory duration of the final planned path and the smoothness cost, respectively.

Scenarios	DGG Computation Time	Planning Time
Pick up a right object (Fig. 3)	32ms	93ms
Dont put on the laptop (Fig. 4)	16ms	98ms
Move around the obstacle (Fig. 5)	16ms	95ms
Static Commands Input (Fig. 6)	73ms	482ms
Dynamic Command Input (Fig. 7)	58ms	427ms

Table 2 Running time (ms) of DGG and motion planning for each scenario on a multi-core PC. Both modules of our approach exhibit realtime performance for HRI and dynamic scenes.

- *Trajectory Duration*: is the duration between the time the first NLP command is given and the time the robot successfully completes the task after trajectory computation. A shorter duration implies higher performance.
- *Trajectory Smoothness Cost*: is based on evaluating the trajectory smoothness based on standard metrics and divide it by the trajectory duration. A lower cost implies a smoother and stable trajectory.

Table 1 shows the results of the experiments with varying number of training data samples on the simulation environment shown in Fig. 3. When the number of training data samples increases, the success rate also increases, and the trajectory duration and the trajectory smoothness cost decrease. Also, the standard deviations also decreases, implying that our planning cost function mapping algorithm becomes more stable. Table 2 shows the running time of our algorithm and the distances from the obstacle on the table in the real world settings.

7.1 Benefits over Prior Methods

Most prior methods that combine NLP and motion planning have focused on understanding natural language instructions computing robot motion for simple environments and constraints. In our approach, the goal is to generate appropriate high-DOF motion trajectory in response to complex natural language commands, as shown in Section 6. Furthermore, our optimization-based formulation is designed to handle challenging scenarios with lot of obstacles and constraints (e.g. dynamics constraints, smoothness constraints), on the resulting trajectories and this results in stable trajectories. Unlike prior methods, the output of NLP parsing algorithm is

directly coupled with the specification of the motion planning problem as a constrained optimization methods. This enables to handle many complex NLP commands including negation, velocity or position constraints or orientation specification. As the parsing capabilities of NLP systems improve in the future, we can map more complex commands to our framework.

8 Limitations, Conclusions and Future Work

We presented a real-time motion planning algorithm that computes appropriate trajectories based on complex NLP commands. We highlight the performance in simulated and real-world scenes with a 7-DOF manipulator operating next to humans. The preliminary results are promising and our approach can handle complex scenarios as compared to prior methods.

We use a trajectory optimization algorithm to compute the high-DOF robot trajectory. It is a high-dimensional optimization problem and the solver get stuck in local minima. As a result, it is hard to provide rigorous guarantees in terms of satisfying all the constraints or following the intent of the user. Furthermore, the accuracy of the mapping algorithm varies as a function of the training data. As future work, we would like to overcome these limitations and evaluate the approach in challenging scenarios with moving obstacles and perform complex robot tasks. More work is needed to handle the full diversity of a natural language, especially for rare words, complicated grammar styles, as well as hidden intention or emotion in the human speech. We plan to incorporate stronger natural language processing and machine learning methods such as those based on semantic parsing, neural sequence-to-sequence models, reinforcement learning, and speech-based emotion analysis, and compute the appropriate optimization-based planning formulations.

References

1. T. Kollar, S. Tellex, M. R. Walter, A. Huang, A. Bachrach, S. Hemachandra, E. Brunskill, A. Banerjee, D. Roy, S. Teller *et al.*, “Generalized grounding graphs: A probabilistic framework for understanding grounded language,” *JAIR*, 2013.
2. T. M. Howard, S. Tellex, and N. Roy, “A natural language planner interface for mobile manipulators,” in *Robotics and Automation (ICRA), 2014 IEEE International Conference on*. IEEE, 2014, pp. 6652–6659.
3. S. R. Branavan, H. Chen, L. S. Zettlemoyer, and R. Barzilay, “Reinforcement learning for mapping instructions to actions,” in *Proceedings of the Joint Conference of the 47th Annual Meeting of the ACL and the 4th International Joint Conference on Natural Language Processing of the AFNLP: Volume 1-Volume 1*. Association for Computational Linguistics, 2009, pp. 82–90.
4. C. Matuszek, D. Fox, and K. Koscher, “Following directions using statistical machine translation,” in *Human-Robot Interaction (HRI), 2010 5th ACM/IEEE International Conference on*. IEEE, 2010, pp. 251–258.

5. S. Branavan, N. Kushman, T. Lei, and R. Barzilay, "Learning high-level planning from text," in *Proceedings of the 50th Annual Meeting of the Association for Computational Linguistics: Long Papers-Volume 1*. Association for Computational Linguistics, 2012, pp. 126–135.
6. F. Duvallet, T. Kollar, and A. Stentz, "Imitation learning for natural language direction following through unknown environments," in *Robotics and Automation (ICRA), 2013 IEEE International Conference on*. IEEE, 2013, pp. 1047–1053.
7. D. Fox, W. Burgard, and S. Thrun, "The dynamic window approach to collision avoidance," *IEEE Robotics & Automation Magazine*, vol. 4, no. 1, pp. 23–33, 1997.
8. M. Zucker, N. Ratliff, A. D. Dragan, M. Pivtoraiko, M. Klingensmith, C. M. Dellin, J. A. Bagnell, and S. S. Srinivasa, "CHOMP: Covariant hamiltonian optimization for motion planning," *International Journal of Robotics Research*, 2012.
9. M. Kalakrishnan, S. Chitta, E. Theodorou, P. Pastor, and S. Schaal, "STOMP: Stochastic trajectory optimization for motion planning," in *Proceedings of IEEE International Conference on Robotics and Automation*, 2011, pp. 4569–4574.
10. M. Zucker, N. Ratliff, A. D. Dragan, M. Pivtoraiko, M. Klingensmith, C. M. Dellin, J. A. Bagnell, and S. S. Srinivasa, "Chomp: Covariant hamiltonian optimization for motion planning," *The International Journal of Robotics Research*, vol. 32, no. 9-10, pp. 1164–1193, 2013.
11. C. Park, J. Pan, and D. Manocha, "ITOMP: Incremental trajectory optimization for real-time replanning in dynamic environments," in *Proceedings of International Conference on Automated Planning and Scheduling*, 2012.
12. D. Silver, J. A. Bagnell, and A. Stentz, "Learning autonomous driving styles and maneuvers from expert demonstration," in *Experimental Robotics*. Springer, 2013, pp. 371–386.
13. E. A. Sisbot, L. F. Marin-Urias, R. Alami, and T. Simeon, "A human aware mobile robot motion planner," *Robotics, IEEE Transactions on*, vol. 23, no. 5, pp. 874–883, 2007.
14. A. D. Dragan, S. Bauman, J. Forlizzi, and S. S. Srinivasa, "Effects of robot motion on human-robot collaboration," in *Proceedings of the Tenth Annual ACM/IEEE International Conference on Human-Robot Interaction*. ACM, 2015, pp. 51–58.
15. J. Mainprice and D. Berenson, "Human-robot collaborative manipulation planning using early prediction of human motion," in *Intelligent Robots and Systems (IROS), 2013 IEEE/RSJ International Conference on*. IEEE, 2013, pp. 299–306.
16. L. Busoniu, R. Babuska, and B. De Schutter, "A comprehensive survey of multiagent reinforcement learning," *Systems, Man, and Cybernetics, Part C: Applications and Reviews, IEEE Transactions on*, vol. 38, no. 2, pp. 156–172, 2008.
17. S. Nikolaidis, P. Lasota, G. Rossano, C. Martinez, T. Fuhlbrigge, and J. Shah, "Human-robot collaboration in manufacturing: Quantitative evaluation of predictable, convergent joint action," in *Robotics (ISR), 2013 44th International Symposium on*. IEEE, 2013, pp. 1–6.
18. H. S. Koppula, A. Jain, and A. Saxena, "Anticipatory planning for human-robot teams," in *Experimental Robotics*. Springer, 2016, pp. 453–470.
19. C. Park, J. Pan, and D. Manocha, "Real-time optimization-based planning in dynamic environments using GPUs," in *Proceedings of IEEE International Conference on Robotics and Automation*, 2013.
20. S. Bird, "Nltk: the natural language toolkit," in *Proceedings of the COLING/ACL on Interactive presentation sessions*. Association for Computational Linguistics, 2006, pp. 69–72.
21. J. Pennington, R. Socher, and C. D. Manning, "Glove: Global vectors for word representation," in *Empirical Methods in Natural Language Processing (EMNLP)*, 2014, pp. 1532–1543. [Online]. Available: <http://www.aclweb.org/anthology/D14-1162>